



## Polarization dependence of atomic high-order harmonic generation: Description using a discrete basis

József Kasza,<sup>1,2</sup> István Magashegyi,<sup>2</sup> Péter Dombi <sup>1,3</sup> and Péter Földi <sup>1,2</sup>

<sup>1</sup>*ELI-ALPS, ELI-HU Non-Profit Limited, Wolfgang Sandner utca 3, H-6728 Szeged, Hungary*

<sup>2</sup>*Department of Theoretical Physics, University of Szeged, Tisza Lajos kör út 84, H-6720 Szeged, Hungary*

<sup>3</sup>*Wigner Research Centre for Physics, Konkoly-Thege M. út 29-33, H-1121 Budapest, Hungary*



(Received 5 November 2021; accepted 28 February 2022; published 14 March 2022)

The optical generation of high-order harmonics is known to have a strong polarization dependence: In contrast to linearly polarized excitation, circularly polarized light induces practically no harmonics. In the current paper we focus on atomic targets, the case when a well-established physical picture explains the effect: For circular polarization, the photoionized electrons never return to their parent nuclei, and the energy they gained while being accelerated by the field is not transferred into high-order harmonic radiation. This is essentially a picture that is based on real-space electron trajectories (or the dynamics of the wave functions). Here, we provide an alternative description that uses the discrete Sturmian basis, and points out how quantum mechanical interference effects and selection rules can explain the polarization dependence of the process. This emphasizes the importance of space-time symmetries during the process of high-order harmonic generation.

DOI: [10.1103/PhysRevA.105.033105](https://doi.org/10.1103/PhysRevA.105.033105)

### I. INTRODUCTION

The highly nonlinear process of generating the high-order harmonics of the central frequency corresponding to a strong optical excitation has already been detected using various physical systems as the target material [1–5]. Besides its own importance in deepening our understanding of the underlying strong-field mechanisms, the phenomenon is fundamental also in laser technology: The emergence of short (even attosecond domain) bursts of electromagnetic radiation is based on the appropriate superposition of the harmonics [6,7]. For gaseous samples, the physical mechanisms that are responsible for the appearance of the harmonics can be understood using a clear, transparent interpretation in terms of the two- or three-step models and their generalizations [8–10]. In short, atomic electrons leave the vicinity of the nuclei as driven by the laser field, accelerate in the field, and in the next optical half cycle, when they return, a part of the energy they gained is transferred to high-order harmonics that are being emitted.

In this picture, the polarization dependence of the high-order harmonic generation (HHG) process is clear: When the exciting field is circularly polarized, the classical electron trajectories never return to the nuclei, leading to the absence of high-order harmonic (HH) radiation. A similar result can be obtained using a quantum mechanical description, when the electrons' dynamics driven by the time-dependent Schrödinger equation show a negligible overlap of the bound and free parts of the wave functions for circular polarization. In fact, the finite spatial extension of the electronic wave packet can explain the gradual disappearance of the high-order harmonics as the degree of ellipticity increased [11,12] (in contrast to results that are based on classical trajectories and predict a sudden transition). The “threshold ellipticity”

[the full width at half maximum (FWHM) of this decay] has also been defined, calculated, and measured [13–17]. For targets larger than single atoms it is interesting to see whether the recombination that is responsible for the generation of the HH radiation still happens locally, or more atoms play a significant role in the process [18]. The understanding of these results is essentially based on a description in the real, three-dimensional space, where a point  $\mathbf{r}$  describes either the time-dependent position of an electron, or the argument of the corresponding wave function.

However, in a quantum mechanical description, position representation is not the only possibility, as we have the freedom to use, e.g., a different, discrete basis. This can provide complementary information, by telling us what quantum mechanical effects lead to the absence of harmonics for circularly polarized exciting fields. As the three-step model shows, the continuum part of the spectrum plays an essential role here, therefore the traditional hydrogenlike bound eigenstates cannot provide an appropriate description. Instead of complementing this set using eigenstates that correspond to the continuum, in the following we apply Sturmian states [19,20], which also form a true basis containing both parts of the spectrum. Expanding the dynamical equations in this basis, we can identify the quantum numbers that determine the polarization dependence of the HHG process. Clearly, each member of the Sturmian basis corresponds to a well-defined wave function, thus our results are physically equivalent to the usual description in real space. The most important benefit of the method to be described in the following is that it can straightforwardly reveal symmetry-related, fundamental aspects of the polarization dependence of HHG.

In the current paper we focus on hydrogenlike systems. First, in Sec. II, the properties of the Sturmian basis are

summarized briefly, then, in Sec. III, we show that the known polarization dependence of the HHG process can be recovered using this basis. In Sec. IV, analytic calculations are presented that explain the quantum mechanical reasons for the observed polarization dependence. Conclusions are drawn in Sec. V.

## II. DYNAMICAL EQUATIONS AND THE STURMIAN BASIS

The Hamiltonian describing the interaction of a hydrogen-like atom and an external laser pulse is given by

$$H(t) = H_0 + V(t), \quad (1)$$

where  $H_0$  denotes the atomic Hamiltonian that has the well-known bound states usually labeled by the quantum numbers  $n$ ,  $l$ , and  $m$ . Using a length gauge and dipole approximation, the interaction with the electric field of the laser can be written as

$$V(t) = -\mathbf{D}\mathbf{E}(t), \quad (2)$$

where  $\mathbf{D}$  denotes the (three-component) dipole moment operator of the atom. In the following we assume that the exciting field is polarized in the  $x$ - $y$  plane, i.e.,  $E_z = 0$ . For elliptically polarized excitation, we use

$$E_x = E_0(t) \cos \omega t \cos \theta, \quad E_y = E_0(t) \sin \omega t \sin \theta, \quad (3)$$

where the envelope  $E_0(t)$  changes slowly on the timescale determined by the cycle time that can be calculated using the central frequency, i.e.,  $T = 2\pi/\omega$ . The angle  $\theta$  provides a continuous transition between  $x$ -direction linear ( $\theta = 0$ ), circular ( $\theta = \pi/4$ ), and  $y$ -direction linear ( $\theta = \pi/2$ ) polarizations. [The parameter  $\epsilon$  (ellipticity: the ratio of the minor and the major axes of the polarization ellipse) that was used, e.g., in Refs. [13,14,18], is given by  $\tan \theta$  for  $\theta \in [0, \pi/4]$  and by  $\cot \theta$  for  $\theta$  between  $\pi/4$  and  $\pi/2$ .] Clearly, Eq. (3) is not the most general possible expression, but for an initial state that is spherically symmetric, it is only the degree of the ellipticity and not the orientation of the polarization ellipse that is relevant. Using Eq. (3), we can investigate the ellipticity dependence of the process of HHG—and can also check the accuracy of our numerical approach by monitoring the orientation independence.

Let us note that Eq. (2) uses dipole approximation and it also means a specific choice of the electromagnetic gauge (namely, the length gauge). The latter fact is not crucial from the viewpoint of the following results, since the selection rules that will be considered are gauge independent. The two facets of dipole approximation, i.e., neglecting both the spatial dependence of the electric field and the influence of the magnetic field, can be summarized as assuming a vector potential that has weak spatial dependence [21] on the characteristic length scale of the interaction. The latter is not trivial to identify during the process of HHG, e.g., the spreading of the electron wave packet that escaped the atom also has to be taken into account [21,22]. However, considering all these aspects, we can conclude that for the parameter range considered in the following, the dipole approximation provides an accurate description of the problem.

In the following, we solve the time-dependent Schrödinger equation induced by the Hamiltonian (1). To this end,

we apply Sturmian states as a basis. Due to the spherical symmetry of the problem, it is convenient to use spherical coordinates  $(r, \vartheta, \phi)$ . With this notation, the wave functions corresponding to the Sturmian states read [19,20]

$$S_{n,l,m}^\alpha(r, \vartheta, \phi) = \frac{\alpha^{3/2} 2^{l+1} e^{-\alpha r}}{(2l+1)!} \sqrt{\frac{(l+n)!}{n(-l+n-1)!}} (\alpha r)^l {}_1F_1 \times (l-n+1; 2l+2; 2\alpha r) Y_l^m(\theta, \phi). \quad (4)$$

Here,  $Y_l^m(\theta, \phi)$  and  ${}_1F_1(l-n+1; 2l+2; 2\alpha r)$  denote the spherical harmonics and the generalized hypergeometric function, respectively. The functions (4) span the complete Hilbert space of the problem, including both bound states with negative energies as well as states in the continuum corresponding to positive energies. This holds for all values of  $\alpha$ . For the sake of definiteness, we use  $\alpha = 1$  in the following, and omit its explicit notation. The orthogonality relation for the Sturmian functions reads

$$\begin{aligned} \langle S_{n,l,m} | S_{n',l',m'} \rangle &= \int S_{n,l,m}^*(\mathbf{r}) \frac{1}{r} S_{n',l',m'}(\mathbf{r}) d^3\mathbf{r} \\ &= \delta_{nn'} \delta_{ll'} \delta_{mm'}, \end{aligned} \quad (5)$$

i.e., the weight function of  $1/r$  has to be inserted in the integrals [20]. In order to perform calculations using the Sturmian basis, the matrix elements of  $H_0$  and  $V(t)$  have to be evaluated using the inner product above. For example, for the  $x$  component of  $\mathbf{D} = e\mathbf{r}$  we need the matrix elements

$$\begin{aligned} X_{nlm}^{n'l'm'} &= \langle S_{n,l,m} | X | S_{n',l',m'} \rangle \\ &= \int S_{n,l,m}^*(\mathbf{r}) \frac{x}{r} S_{n',l',m'}(\mathbf{r}) d^3\mathbf{r} \\ &= \int_0^{2\pi} \int_0^\pi \int_0^\infty S_{n,l,m}^*(r, \vartheta, \phi) \sin \vartheta \cos \phi \\ &\quad \times S_{n',l',m'}(r, \vartheta, \phi) r^2 \sin \vartheta dr d\vartheta d\phi. \end{aligned} \quad (6)$$

(Note that using both subscripts and superscripts is just a matter of convenience here, and  $e$  denotes the charge of an electron, including the sign.) For numerical calculations, the number of the Sturmian functions that we can use is obviously finite. For the expansion of energy eigenstates corresponding to the principal quantum numbers of  $n = 1, 2$ , and  $3$ , only a few Sturmian states are needed. In the following, the lowest-energy eigenstate (the ground state) will be the initial state of the time evolution. We also checked the convergence of the dynamics, i.e., increased the size of the truncated Sturmian basis until the results did not change observably.

## III. POLARIZATION DEPENDENCE OF THE HHG SPECTRA

Having obtained the matrix elements of the Hamiltonian (1) in the Sturmian basis, we can calculate the time evolution induced by external fields with peak intensities in the  $10^{12}$ - $10^{14}$  W/cm<sup>2</sup> range. That is, we determine the time-dependent coefficients in the expansion  $|\Psi\rangle(t) = \sum c_{nlm}(t) |S_{n,l,m}\rangle$ , with the initial state being one of the

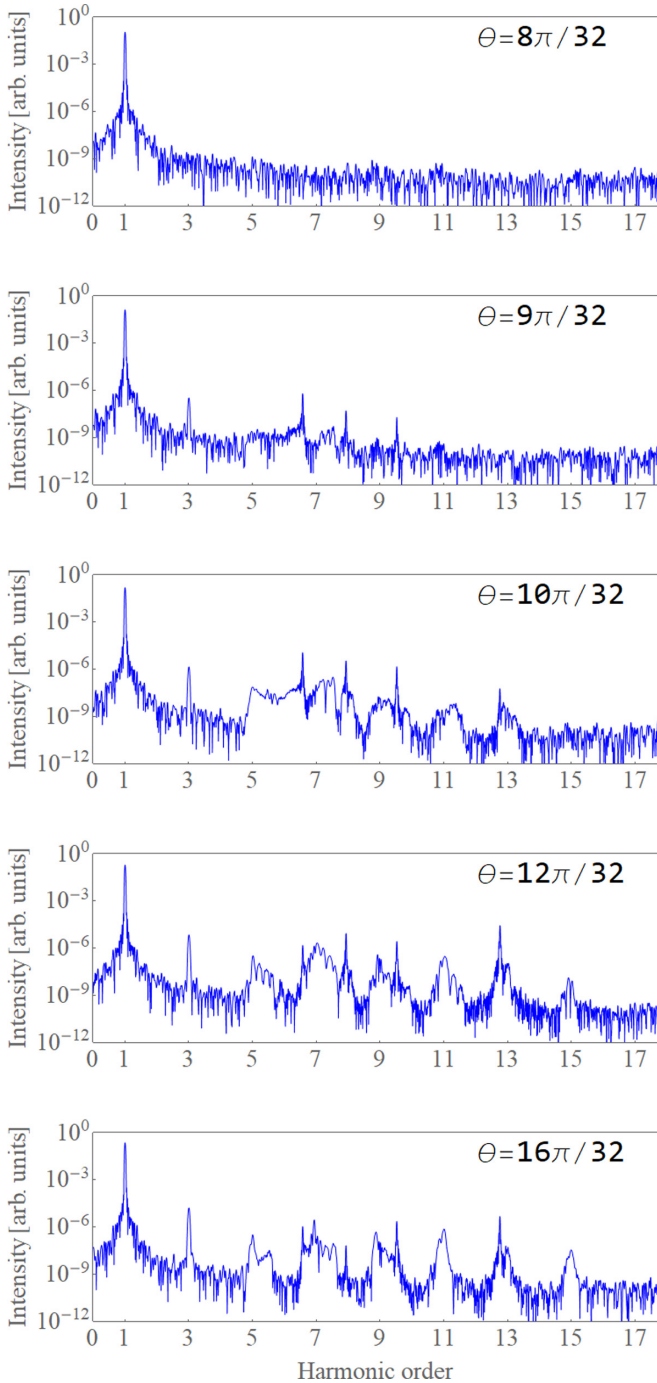


FIG. 1. Power spectra of  $\langle D_y \rangle(t)$  for different values of  $\theta$  in Eq. (3). The ellipticity is  $\epsilon = 1$  for the top panel and it gradually decreases to zero (bottom panel). Note that the scale of the vertical axis is logarithmic. Parameters:  $E_0 = 0.025$  (atomic units), central wavelength  $\lambda = 800$  nm,  $\tau/T = 50$ , which corresponds to approximately 18 optical cycles (intensity FWHM).

eigenstates  $|n, l, m\rangle$ . The time-dependent Schrödinger equation using this basis reads

$$i\hbar \frac{d}{dt} c_{nlm}(t) = \sum_{n', l', m'} H_{nlm}^{n'l'm'}(t) c_{n'l'm'}(t). \quad (7)$$

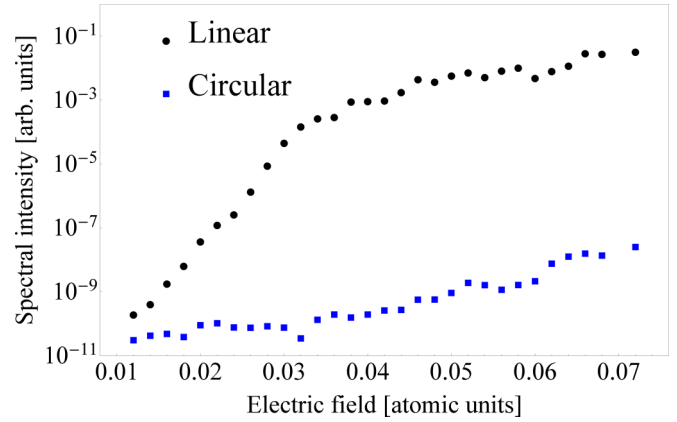


FIG. 2. The height of the ninth harmonic peak as a function of the amplitude of the exciting field  $E_0$ . The central wavelength is  $\lambda = 800$  nm,  $\tau/T = 50$ , which corresponds to approximately 18 optical cycles (intensity FWHM). Note that the scale of the vertical axis is logarithmic.

For the temporal envelope of the exciting field we use the following,

$$E_0(t) = E_0 \sin^2 \frac{\pi t}{\tau}, \quad (8)$$

provided  $t \in [0, \tau]$ , and zero otherwise. In order to obtain strong, well-defined high-order harmonic peaks in the spectra, we focus on multicycle pulses, i.e., to the range  $\tau \gg 2\pi/\omega = T$ . In the numerical calculations we consider a realistic  $\lambda = Tc = 800$  nm central wavelength.

As expected, when the initial atomic state is the spherically symmetric ground state, the time evolution (and consequently the power spectra) of the dipole moment operators is also symmetric:  $\langle D_x \rangle(t)$  for a given  $\theta$  [see Eq. (3)] is numerically the same as  $\langle D_y \rangle(t)$  for  $\theta' = \pi/4 - \theta$ , which corresponds to the same ellipticity but different orientation of the polarization ellipse. Therefore it is sufficient to consider the power spectra of, e.g.,  $\langle D_y \rangle(t)$  for  $\theta \in [\pi/4, \pi/2]$ . As we can see in Fig. 1, changing the excitation from a linearly to elliptically and finally to a circularly polarized field, leads to the gradual disappearance of the high-order harmonic peaks in the power spectra of the secondary radiation emitted by the atom. All these results are in agreement with the expectations as well as with known experimental results, and thus confirm the validity of this model.

Figure 1 corresponds to a single amplitude of the exciting field, but calculations for different values of  $E_0$  were also performed (see Fig. 2), which—as an example—shows the height of a single HH peak (the ninth one) for both linearly and circularly polarized excitations. As we can see, the HH signal is always weaker for circularly polarized excitation than for the linear case. In fact, although the former is also increasing with  $E_0$ , it is practically on the level of the numerical noise. On the other hand, for linearly polarized excitation, the increase of the HH signal is pronounced, and the difference between the multiphoton and tunnel ionization regimes can also be seen. (The strongest field amplitude in the figure corresponds to a Keldysh parameter slightly below 0.8.) When the external field is strong enough to induce observable HH radiation, there

is a several orders of magnitude difference between the signals for linearly and circularly polarized excitations.

Although it is clearly not an effective way of generating elliptically polarized HH radiation, it is interesting to note that for elliptically polarized excitation, when HH peaks are observable, the high-order harmonic radiation is also elliptically polarized. Details of the methods that can efficiently generate elliptically or circularly polarized harmonics can be found, e.g., in Refs. [23–27].

For the case of precisely circularly polarized excitation, it is instructive to investigate, whether the high-order harmonics are completely absent (there is nothing that oscillates at these frequencies during the quantum mechanical time evolution) or it is just the measurable secondary radiation that contains no harmonics. Our calculations are in accord with the second case: The power spectra of the coefficients  $c_{nlm}(t)$  show clear signatures of the HH peaks. This means a certain presence of the HH frequencies, which are, however, not being radiated. The reasons for that will be shown in the next section.

#### IV. EXPLAINING THE RESULTS USING THE STURMIAN BASIS

The interaction Hamiltonian for circularly polarized excitation corresponds to the cases of  $\theta = \pi/4 \pmod{\pi}$  in Eq. (3). In the following we choose  $\theta = \pi/4$  (“left circular polarization”):

$$E_x = \frac{E_0(t)}{\sqrt{2}} \cos \omega t, \quad E_y = \frac{E_0(t)}{\sqrt{2}} \sin \omega t. \quad (9)$$

This leads to the following expression for the interaction term in Eq. (1),

$$V(t) = -e \frac{E_0(t)}{\sqrt{2}} (X \cos \omega t + Y \sin \omega t), \quad (10)$$

where coordinate operators appear on the right-hand side. Note that all the calculations below can be repeated with straightforward modifications for right circular polarization. Let us introduce

$$X_{\pm} = X \pm iY, \quad (11)$$

which satisfy  $X_{\pm}^{\dagger} = X_{\mp}$ . These operators allow us to rewrite Eq. (10) as

$$V(t) = -\frac{eE_0(t)}{2\sqrt{2}} (X_+ e^{-i\omega t} + X_- e^{i\omega t}). \quad (12)$$

The matrix elements of  $X_{\pm}$  and the selection rules in the Sturmian basis can be determined using the fact that the orientation dependence of the Sturmian functions is the same as that of the usual hydrogen eigenfunctions, i.e., orbital angular momentum eigenfunctions  $Y_{lm}(\theta, \phi)$  appear in both cases. In view of this, we have

$$\langle S_{n,l,m} | X_{\pm} | S_{n',l',m'} \rangle = 0, \quad (13)$$

unless  $m' = m - 1$ . Similarly, the matrix elements  $\langle S_{n,l,m} | X_{\mp} | S_{n',l',m'} \rangle$  are nonzero, only if  $m' = m + 1$ . (The simplest way of proving this is using the commutation relation  $[L_z, X_{\pm}] = \pm \hbar X_{\pm}$  combined with fact that  $L_z | S_{n,l,m} \rangle = \hbar m | S_{n,l,m} \rangle$ . Since the same calculation can be carried out using the components of the momentum

operator instead of that of position, we can explicitly see that the selection rules are the same using both the length and velocity gauges.)

For the sake of simplicity, let us consider monochromatic excitation [ $E_0(t) = E_0$ ] from now on. In this case it is worth introducing a time-dependent Sturmian-Floquet basis [28],

$$|S_{n,l,m}; k\rangle = |S_{n,l,m}\rangle |k\rangle = |S_{n,l,m}\rangle e^{ik\omega t}, \quad (14)$$

with  $k$  being an integer (and  $|k\rangle$  is simply an abstract notation for  $\exp ik\omega t$  that was introduced to simplify the equations to come). Since for constant  $E_0$  the Hamiltonian is periodic in time (with a cycle time of  $T = 2\pi/\omega$ ), general results [29] tell us that the solutions of the corresponding time-dependent Schrödinger equation can be searched in the following form,

$$|\varphi_j\rangle(t) = e^{-i\frac{\varepsilon_j}{\hbar}t} |u_j\rangle(t), \quad (15)$$

where the Floquet states satisfy  $|u_j\rangle(t) = |u_j\rangle(t + T)$ . The set  $\{|\varphi_j\rangle(t)\}$  can be considered to form a time-dependent basis, and by superposition, the states  $|\varphi_j\rangle(t)$  can be used to construct any solution of the time-dependent Schrödinger equation. In principle, the corresponding linear combinations contain infinite terms, but for practical purposes, the sum can be truncated. The standard way of finding the states  $|u_j\rangle$  and the Floquet quasienergies  $\varepsilon_j$  is by solving the eigenvalue equation  $H_F |u_j\rangle = \varepsilon_j |u_j\rangle$ , where the Floquet Hamiltonian  $H_F$  does not depend on time, and can be defined via its action,

$$H_F |S_{n,l,m}; k\rangle = [(H_0 + k\hbar\omega) |S_{n,l,m}\rangle] |k\rangle - \frac{eE_0}{2} (X_+ |S_{n,l,m}\rangle \times |k-1\rangle + X_- |S_{n,l,m}\rangle |k+1\rangle). \quad (16)$$

The selection rules together with the form (12) of  $V(t)$  lead to the conservation of the sum of the indices  $m$  and  $k$ . (Since  $H_0$  changes none of these indices, it trivially conserves  $m + k$ .) This means that the Floquet Hamiltonian above has invariant subspaces that can be labeled by  $N = m + k$ . That is, the eigenvalue problem of  $H_F$  decomposes to sets of equations  $H_F |u_{j,N}\rangle = \varepsilon_{j,N} |u_{j,N}\rangle$ , that are independent for different values of  $N$ . Different values of  $N$ , however, do not provide physically different solutions: As we can see easily, although  $|u_{j,N}\rangle(t) e^{i\omega t}$  and  $\varepsilon_{j,N} + \hbar\omega$  correspond to the subspace labeled by  $N + 1$  (i.e., they can be identified with  $|u_{j,N+1}\rangle(t)$  and  $\varepsilon_{j,N+1}$ ), the time-dependent Floquet solutions  $\exp(-i\varepsilon_{j,N}) |u_{j,N}\rangle$  and  $\exp(-i\varepsilon_{j,N+1}) |u_{j,N+1}\rangle$  are the same. Therefore it is sufficient to consider a single value of  $N$ , which, for the sake of simplicity, can be zero. That is, a general solution of the original time-dependent Schrödinger equation can be written as

$$|\Psi\rangle(t) = \sum_j e^{-i\frac{\varepsilon_j}{\hbar}t} \sum_{n,l,m} \alpha_{n,l,m}^j |S_{n,l,m}\rangle |k = -m\rangle, \quad (17)$$

where the coefficients  $\alpha$  are to be determined using the initial conditions. Equation (17) shows that the condition  $k = -m$  means that the spatial and temporal parts of the state are entangled. Now let us calculate the expectation value of the dipole moment operator in this general solution. As an example, for



the  $x$  component, we have

$$\begin{aligned} \langle D_x \rangle(t) = & e \sum_{j,n,l,m} \sum_{j',n',l',m'} e^{i \frac{\epsilon_j - \epsilon_{j'}}{\hbar} t + i(m-m')\omega t} \\ & \times X_{nlm}^{n'l'm'} \alpha_{n',l',m'}^{j'} (\alpha_{n,l,m}^j)^*. \end{aligned} \quad (18)$$

On the other hand,  $X = (X_+ + X_-)/2$  has nonzero matrix elements only if  $m' = m \pm 1$ . That leads to time-dependent factors of  $\exp(i \frac{\epsilon_j - \epsilon_{j'}}{\hbar} t + i\omega t)$  and  $\exp(i \frac{\epsilon_j - \epsilon_{j'}}{\hbar} t - i\omega t)$ . Since generally the difference  $\frac{\epsilon_j - \epsilon_{j'}}{\hbar}$  is not an integer multiple of the exciting frequency  $\omega$ , we see that high-order harmonics are completely missing from the spectrum. [The expression for  $\langle D_y \rangle(t)$  is similar to Eq. (18).] Let us recall that the terms  $|k = -m\rangle$  in Eq. (17) mean exponential factors  $\exp(im\omega t)$ , i.e., the presence of high-order harmonics in the general solution  $|\Psi\rangle(t)$ . On the other hand, when the expectation values  $\langle D_x \rangle(t)$  and  $\langle D_y \rangle(t)$  are calculated, the selection rules and the spatiotemporal entanglement lead to the disappearance of the harmonics.

It is interesting to note that the expression (12) is formally analogous to the light-matter interaction term that appears in the classical Rabi problem (or a two-level atom in a monochromatic classical external field) with the usage of the rotating-wave approximation (RWA) [30]. [Formally, apart from the prefactors, the Rabi interaction term can be obtained by replacing  $X_{\pm}$  by  $\sigma_{\pm}$  in Eq. (12), where  $\sigma_+$  ( $\sigma_-$ ) represents an upward (downward) atomic transition.] Using RWA, the problem is analytically solvable, and we recall that no high-order harmonics appear in this case, independently from the amplitude of the driving field. Let us also note that RWA is exact for the Rabi problem in the case of circularly polarized exciting field. This means that there are no high-order harmonics for circularly polarized excitation—already in a model as simple as a two-level atom.

It is also worth considering an analogy with the case of a two-level atom in a quantized, single-mode electromagnetic field, i.e., with the Jaynes-Cummings-Paul model [30]. Note that the quantum optical description of the process of HHG has recently gained considerable attention. For experimental results, see Refs. [31,32], while theoretical models can be found, e.g., in Refs. [33–36]. In this picture, the Hamiltonian for circularly polarized excitation reads

$$H_q = \hbar\omega a^\dagger a + H_0 - e\mathcal{E}_0(X_+ a + X_- a^\dagger), \quad (19)$$

where  $a$  and  $a^\dagger$  denote the annihilation and creation operator of the circularly polarized mode, and  $\mathcal{E}_0 = \sqrt{\frac{\hbar\omega}{\epsilon_0\mathcal{V}}}$ , with  $\mathcal{V}$  being the quantization volume and  $\epsilon_0$  denoting the vacuum permittivity. The last term in this Hamiltonian [the quantized version of Eq. (12)] is very instructive: The conserved quantity now is the sum of the photon numbers in the exciting field and the atomic angular momentum index  $m$ . However, for circular excitation (with the helicity corresponding to the case we investigated so far), each photon carries an angular momentum of  $\hbar$ . Considering this, and the selection rules for  $X_{\pm}$ , the term  $X_+ a + X_- a^\dagger$  simply expresses the conservation of angular momentum: In line with the creation of a photon with helicity of  $\hbar$ , the atomic orbital angular momentum is decreased by the same amount, and vice versa. In view of this, it is a fundamental conservation law that hinders the appearance of high-order harmonics for circularly polarized excitation.

Let us note that the results of the current section were obtained by assuming a monochromatic external field, which is clearly an approximation when we consider excitations with laser pulses. However, for long, many-cycle pulses, our results are in complete agreement with the numerical calculations of the previous section as well as with experimental results.

## V. CONCLUSIONS

We considered the process of atomic high-order harmonic generation, and introduced a description that is complementary to the usual, real-space picture. Instead of focusing on the position dependence of the wave functions, we expanded the dynamical equations in the Sturmian basis. This allowed us to point out that it is essentially the conservation of angular momentum that is responsible for the absence of the high-order harmonics for circularly polarized excitation.

## ACKNOWLEDGMENTS

Partial support by the ELI-ALPS project is acknowledged. The ELI-ALPS project (GINOP-2.3.6-15-2015-00001) is supported by the European Union and cofinanced by the European Regional Development Fund. We also acknowledge financial support by Grant No. TUDFO/47138-1/2019-ITM FIKP of the Ministry of Innovation and Technology, Hungary. This work was also supported by the National Research, Development and Innovation Office of Hungary with projects VEKOP-2.3.2-16-2017-00015 and 2018-1.2.1-NKP-2018-00012.

- 
- [1] M. Ferray, A. L’Huillier, X. F. Li, L. A. Lompre, G. Mainfray, and C. Manus, Multiple-harmonic conversion of 1064 nm radiation in rare gases, *J. Phys. B: At., Mol. Opt. Phys.* **21**, L31 (1988).
- [2] A. L’Huillier and P. Balcou, High-Order Harmonic Generation in Rare Gases with a 1-ps 1053-nm Laser, *Phys. Rev. Lett.* **70**, 774 (1993).
- [3] C.-G. Wahlström, J. Larsson, A. Persson, T. Starczewski, S. Svanberg, P. Salières, P. Balcou, and A. L’Huillier, High-order

- harmonic generation in rare gases with an intense short-pulse laser, *Phys. Rev. A* **48**, 4709 (1993).
- [4] S. Ghimire, A. D. DiChiara, E. Sistrunk, P. Agostini, L. F. DiMauro, and D. A. Reis, Observation of high-order harmonic generation in a bulk crystal, *Nat. Phys.* **7**, 138 (2011).
- [5] G. A. Reider, XUV attosecond pulses: Generation and measurement, *J. Phys. D* **37**, R37 (2004).
- [6] G. Farkas and C. Tóth, Proposal for attosecond light pulse generation using laser induced multiple-harmonic conver-

- sion processes in rare gases, *Phys. Lett. A* **168**, 447 (1992).
- [7] F. Krausz and M. Ivanov, Attosecond physics, *Rev. Mod. Phys.* **81**, 163 (2009).
- [8] K. J. Schafer, B. Yang, L. F. DiMauro, and K. C. Kulander, Above Threshold Ionization Beyond the High Harmonic Cutoff, *Phys. Rev. Lett.* **70**, 1599 (1993).
- [9] P. B. Corkum, Plasma Perspective on Strong Field Multiphoton Ionization, *Phys. Rev. Lett.* **71**, 1994 (1993).
- [10] M. Lewenstein, P. Balcou, M. Y. Ivanov, A. L'Huillier, and P. B. Corkum, Theory of high-harmonic generation by low-frequency laser fields, *Phys. Rev. A* **49**, 2117 (1994).
- [11] N. Hay, R. de Nalda, T. Halfmann, K. J. Mendham, M. B. Mason, M. Castillejo, and J. P. Marangos, High-order harmonic generation from organic molecules in ultra-short pulses, *Eur. Phys. J. D* **14**, 231 (2001).
- [12] A. Flettner, J. König, M. B. Mason, T. Pfeifer, U. Weichmann, and G. Gerber, Atomic and molecular high-harmonic generation: A comparison of ellipticity dependence based on the three-step model, *J. Mod. Opt.* **50**, 529 (2003).
- [13] V. V. Strelkov, Theory of high-order harmonic generation and attosecond pulse emission by a low-frequency elliptically polarized laser field, *Phys. Rev. A* **74**, 013405 (2006).
- [14] V. V. Strelkov, M. A. Khokhlova, A. A. Gonoskov, I. A. Gonoskov, and M. Y. Ryabikin, High-order harmonic generation by atoms in an elliptically polarized laser field: Harmonic polarization properties and laser threshold ellipticity, *Phys. Rev. A* **86**, 013404 (2012).
- [15] H. Ruf, C. Handschin, R. Cireasa, N. Thiré, A. Ferré, S. Petit, D. Descamps, E. Mével, E. Constant, V. Blanchet, B. Fabre, and Y. Mairesse, Inhomogeneous High Harmonic Generation in Krypton Clusters, *Phys. Rev. Lett.* **110**, 083902 (2013).
- [16] E. W. Larsen, S. Carlström, E. Lorek, C. M. Heyl, D. Paleček, K. J. Schafer, A. L'Huillier, D. Zigmantas, and J. Mauritsson, Sub-cycle ionization dynamics revealed by trajectory resolved, elliptically-driven high-order harmonic generation, *Sci. Rep.* **6**, 39006 (2016).
- [17] P. M. Abanador, F. Mauger, K. Lopata, M. B. Gaarde, and K. J. Schafer, Semiclassical modeling of high-order harmonic generation driven by an elliptically polarized laser field: The Role of recolliding periodic orbits, *J. Phys. B: At., Mol. Opt. Phys.* **50**, 035601 (2017).
- [18] B. Bódi, M. Aladi, P. Rácz, I. B. Földes, and P. Dombi, High harmonic generation on noble gas clusters, *Opt. Express* **27**, 26721 (2019).
- [19] J. Avery and J. Avery, *Generalized Sturmians and Atomic Spectra* (World Scientific, Singapore, 2006).
- [20] J. E. Avery and J. S. Avery, The generalized Sturmian method, in *Solving the Schrödinger Equation: Has Everything Been Tried?* edited by P. Popelier (Imperial College Press, London, 2011), pp. 111–140.
- [21] J. R. Vázquez de Aldana, N. J. Kylstra, L. Roso, P. L. Knight, A. Patel, and R. A. Worthington, Atoms interacting with intense, high-frequency laser pulses: Effect of the magnetic-field component on atomic stabilization, *Phys. Rev. A* **64**, 013411 (2001).
- [22] A. S. Emelina, M. Y. Emelin, and M. Y. Ryabikin, On the possibility of the generation of high harmonics with photon energies greater than 10 keV upon interaction of intense mid-IR radiation with neutral gases, *Quantum Electron.* **44**, 470 (2014).
- [23] J. Levesque, Y. Mairesse, N. Dudovich, H. Pépin, J.-C. Kieffer, P. B. Corkum, and D. M. Villeneuve, Polarization State of High-Order Harmonic Emission from Aligned Molecules, *Phys. Rev. Lett.* **99**, 243001 (2007).
- [24] X. Zhou, R. Lock, N. Wagner, W. Li, H. C. Kapteyn, and M. M. Murnane, Elliptically Polarized High-Order Harmonic Emission from Molecules in Linearly Polarized Laser Fields, *Phys. Rev. Lett.* **102**, 073902 (2009).
- [25] O. Kfir, P. Grychtol, E. Turgut, R. Knut, D. Zusin, D. Popmintchev, T. Popmintchev, H. Nembach, J. M. Shaw, A. Fleischer, H. Kapteyn, M. Murnane, and O. Cohen, Generation of bright phase-matched circularly-polarized extreme ultraviolet high harmonics, *Nat. Photonics* **9**, 99 (2015).
- [26] T. Fan, P. Grychtol, R. Knut, C. Hernández-García, D. D. Hickstein, D. Zusin, C. Gentry, F. J. Dollar, C. A. Mancuso, C. W. Hogle, O. Kfir, D. Legut, K. Carva, J. L. Ellis, K. M. Dorney, C. Chen, O. G. Shpyrko, E. E. Fullerton, O. Cohen, P. M. Oppeneer *et al.*, Bright circularly polarized soft x-ray high harmonics for x-ray magnetic circular dichroism, *Proc. Natl. Acad. Sci. U.S.A.* **112**, 14206 (2015).
- [27] C. Zhai, R. Shao, P. Lan, B. Wang, Y. Zhang, H. Yuan, S. M. Njoroge, L. He, and P. Lu, Ellipticity control of high-order harmonic generation with nearly orthogonal two-color laser fields, *Phys. Rev. A* **101**, 053407 (2020).
- [28] J. Kasza, P. Dombi, and P. Földi, Sturmian-Floquet approach to high-order harmonic generation, *J. Opt. Soc. Am. B* **35**, A126 (2018).
- [29] G. Floquet, Sur les équations différentielles linéaires a coefficients périodiques, *Ann. École Norm. Sup.* **12**, 46 (1883).
- [30] P. Meystre and M. Sargent, *Elements of Quantum Optics*, 2nd ed. (Springer, Berlin, 1991).
- [31] N. Tsatrafyllis, I. K. Kominis, I. A. Gonoskov, and P. Tzallas, High-order harmonics measured by the photon statistics of the infrared driving-field exiting the atomic medium, *Nat. Commun.* **8**, 15170 (2017).
- [32] N. Tsatrafyllis, S. Kühn, M. Dumergue, P. Földi, S. Kahaly, E. Cormier, I. A. Gonoskov, B. Kiss, K. Varju, S. Varro, and P. Tzallas, Quantum Optical Signatures in a Strong Laser Pulse after Interaction with Semiconductors, *Phys. Rev. Lett.* **122**, 193602 (2019).
- [33] I. Gonoskov, N. Tsatrafyllis, I. Kominis, and P. Tzallas, Quantum optical signatures in strong-field laser physics: Infrared photon counting in high-order-harmonic generation, *Sci. Rep.* **6**, 32821 (2016).
- [34] A. Gombkötő, A. Czirják, S. Varró, and P. Földi, Quantum-optical model for the dynamics of high-order-harmonic generation, *Phys. Rev. A* **94**, 013853 (2016).
- [35] A. Gorbach, O. Neufeld, N. Rivera, O. Cohen, and I. Kaminer, The quantum-optical nature of high harmonic generation, *Nat. Commun.* **11**, 4598 (2020).
- [36] A. Gombkötő, S. Varró, P. Mati, and P. Földi, High-order harmonic generation as induced by a quantized field: Phase-space picture, *Phys. Rev. A* **101**, 013418 (2020).